

---

# Data-Efficient Reinforcement Learning in Continuous-State POMDPs

---

Rowan McAllister  
Carl Rasmussen

RTM26@CAM.AC.UK  
CER54@CAM.AC.UK

Department of Engineering, University of Cambridge, Cambridge, CB2 1PZ

## Abstract

We present a data-efficient reinforcement learning algorithm resistant to observation noise. Our method extends the highly data-efficient PILCO algorithm (Deisenroth & Rasmussen, 2011) into partially observed Markov decision processes (POMDPs) by considering the filtering process during policy evaluation. PILCO conducts policy search, evaluating each policy by first predicting an analytic distribution of possible system trajectories. We additionally predict trajectories w.r.t. a filtering process, achieving significantly higher performance than combining a filter with a policy optimised by the original (unfiltered) framework. Our test setup is the cartpole swing-up task with sensor noise, which involves nonlinear dynamics and requires nonlinear control.

## 1. Introduction

Real world control systems rely on imperfect sensors to control processes where poor performance often causes real world expense. Learning to control such a system thus entails: 1) an inability to know the state of the system with certainty and, 2) penalties for data-inefficiency.

### 1.1. Data Efficiency

Most reinforcement learning (RL) methods are data-intensive, requiring much system interaction before learning good policies. For systems prone to wear and tear, or expensive to operate, data-efficiency is critical. Model-based RL methods learn models of the unknown system dynamics. They are generally more data-efficient than model-free RL because they 1) generalise local dynamics knowledge, and 2) allow local value backups to propagate globally through state-action space. Unfortunately, a common problem in model-based RL is model bias. Model bias typically arises when predictions are based on a single model selected from a large plausible set, and then assuming the model is correct with certainty. An example is using the maximum a posteriori (MAP) model. Basing predictions

off a single model leaves an RL method susceptible to model error. Any single model is quite possibly the wrong model, being just one of the many plausible explanations of what generated the observed data. And the less data observed, the greater the number of plausible dynamics models. When optimising data-efficiency, the agent constantly learns and acts in the low data regime where the set of plausible models is vast, exacerbating model bias effects. This regime undermines traditional trajectory-based control approaches which assume model-correctness, such as model predictive control or iterative linear quadratic regulators. Unless model-based RL algorithms consider the complete set of plausible dynamics, they will succumb to model-bias, counteracting the data-efficiency benefits of using a model.

PILCO is a model-based RL algorithm which achieved unprecedented data-efficiency in learning to control the cartpole swing-up problem whilst only scaling linearly with horizon (Deisenroth & Rasmussen, 2011). The key to PILCO's success is its *probabilistic* dynamics model, which makes predictions by marginalising over the complete set of plausible dynamics functions. By additionally propagating model uncertainty throughout trajectory prediction PILCO avoids model bias. As a result, PILCO more likely collects data in promising areas of the state space.

### 1.2. Sensor Noise

The reality of imperfect noisy sensors impairs the control of dynamical systems. Such problems can be framed mathematically by partially observable Markov decision processes (POMDPs). Solving a POMDP is more complex than its fully observable counterpart, the MDP (Smallwood & Sondik, 1973). A common approximation to small-noise POMDP problems is to ignore noise. This assumes full observability by learning and planning in observation space rather than latent state space. However, such approximations break down under larger noise levels. For example, consider the cartpole system (Figure 3). Stabilising the pendulum upright requires a controller with a large gain associated with the pendulum angle. This enables the cart to move quickly under the pendulum's centre of gravity in response to slight angle variations. When in-

correctly modelled as a MDP noise associated with reading the pendulum’s angle is injected directly into the policy. The noise is then *amplified* by the high gain, which produces large variation in controller output, quickly destabilising the system.

The negative effects of sensor noise can be mitigated using an observation model and filtering. To *filter* a sequence of sensory outputs is to maintain a belief posterior distribution over the latent system state conditioned on the complete history of previous actions and observations. Implementing a filter is straightforward when the system dynamics are *known* and *linear*, referred to as Kalman filtering. For nonlinear systems, the extended Kalman filter (EKF) is often adequate, as long as the dynamics are *locally linear*, meaning approximately linear within the region covered by the belief distribution. Otherwise, the EKF’s first order Taylor expansion approximation breaks down. Greater nonlinearities usually warrant the unscented Kalman filter (UKF) or particle methods (Ko & Fox, 2009; Ross et al., 2008). The UKF uses a deterministic sampling technique to estimate moments. However, if moments can be computed analytically and exactly, moment-matching methods are preferred. Moment-matching using distributions from the exponential family (e.g. Gaussians) is equivalent to optimising the Kullback-Leibler divergence  $KL(p||q)$  between the true distribution  $p$  and an approximate distribution  $q$ . In such cases, moment-matching is less susceptible to model bias than the EKF due to its conservative predictions (Deisenroth & Peters, 2012).

### 1.3. Related Work

Unfortunately, the literature does not provide a method that is both data efficient and resistant to noise when dynamics are *unknown* and *locally nonlinear*. The original PILCO, which assumes full state observability, fails under moderate sensor noise. One proposed solution is to filter observations during policy execution (Deisenroth & Peters, 2012). Filtering during execution does indeed improve performance, which we demonstrate later. However, without also predicting system trajectories w.r.t. the filtering process, the above method merely optimises policies for unfiltered control, not for filtered control. The mismatch between unfiltered-prediction and filtered-execution restricts PILCO’s ability to take full advantage of filtering. Dallaire et al. (2009) optimise a policy using a more realistic filtered-prediction. However, the method neglects model uncertainty by only using the MAP model. Unlike the method of Deisenroth & Peters (2012), Dallaire et al.’s work (2009) is therefore highly susceptible to model error, hampering data-efficiency.

We propose the best of both worlds by extending PILCO from MDPs to POMDPs using full probabilistic predic-

tions w.r.t. a filtered process. We predict using closed loop filtered control precisely because we execute closed loop filtered control. The resulting policies are thus optimised for the specific case in which they are used. Doing so, our method retains the same data-efficiency properties of PILCO whilst more resistant to observation noise than PILCO. To evaluate our method, we use the benchmark cartpole swing-up task with noisy sensors. We show realistic and probabilistic prediction (to consider uncertainty) helps our method outperform the aforementioned methods.

This paper proceeds by summarising the PILCO framework in greater detail (Section 2), which we modify and extend for application to POMDPs (Section 3). We then compare our method with the aforementioned methods in the cartpole swing-up problem (Section 4), discussing each method’s predicted and empirical performance (Section 5).

## 2. The PILCO Algorithm

PILCO is a model-based policy-search RL algorithm. It applies to continuous-state, continuous-action, continuous-observation and discrete-time control tasks. A probabilistic dynamics model is used to predict one-step system dynamics (from one timestep to the next). This allows PILCO to probabilistically predict multi-step system trajectories over arbitrary time horizons  $T$ , by repeatedly using the predictive dynamics model’s output at one timestep, as the (uncertain) input in the following timestep. For tractability PILCO uses moment-matching to keep the latent state distribution Gaussian. The result is an analytic distribution of system trajectories, approximated as a joint Gaussian distribution over  $T$  states. The policy is evaluated as the expected total cost of the trajectories. Next, the policy is improved using local gradient-based optimisation, searching over policy-parameter space. A distinct advantage of moment-matched prediction for policy search instead of particle methods is smoother policy gradients and less local optima (McHutchon, 2014). Finally, the policy is executed, generating new data to re-train the dynamics model. The whole process then repeats until policy convergence.

For the remainder of this section we discuss, step by step, PILCO summarised by Algorithm 1. We first define a policy  $\pi$  as a parametric function (Algorithm 1, line 1) and initialise the policy parameters  $\psi$  randomly (line 2) since we begin without any data.

### 2.1. System Execution

With a policy now defined, PILCO is ready to *execute* the system (Algorithm 1, line 4). Let the latent state of the system at time  $t$  be  $x_t \in \mathbb{R}^D$ , which is noisily observed as  $z_t = x_t + \epsilon_t$ , where  $\epsilon_t \stackrel{iid}{\sim} \mathcal{N}(0, \Sigma^\epsilon)$ . The policy  $\pi$ , parameterised by  $\psi$ , takes observation  $z_t$  as input, and outputs a

control action  $u_t = \pi(z_t, \psi) \in \mathbb{R}^F$ . Applying action  $u_t$  to the dynamical system in state  $x_t$ , results in a new system state  $x_{t+1}$ . This completes the description of system execution, resulting in a single system-trajectory up until horizon  $T$ .

## 2.2. Learning Dynamics

To model and learn the unknown dynamics (Algorithm 1, line 5), any probabilistic model flexible enough to capture the complexity of the dynamics can be used. Bayesian non-parametric models are particularly suitable because of their resistance to both overfitting and underfitting respectively. Overfitting otherwise leads to model bias, and underfitting limits the complexity of the system this method can learn to control. In a nonparametric model no prior dynamics knowledge is required, not even knowledge of *how complex* the unknown dynamics might be since the model’s complexity can grow with the available data. PILCO chooses to place a Gaussian process (GP) prior on the latent dynamics function  $f$ . The training inputs are state-action pairs:

$$\tilde{x}_t \doteq \begin{bmatrix} x_t \\ u_t \end{bmatrix} \in \mathbb{R}^{D+F}, \quad (1)$$

and targets are noisy observations of resultant states<sup>1</sup>,  $z_{t+1}$ . The covariance function is a square exponential,

$$k(\tilde{x}_i, \tilde{x}_j) = \sigma_f^2 \exp\left(-\frac{1}{2}(\tilde{x}_i - \tilde{x}_j)^\top \Lambda^{-1}(\tilde{x}_i - \tilde{x}_j)\right), \quad (2)$$

with length scales  $\Lambda = \text{diag}([l_1^2, \dots, l_{D+F}^2])$ , and signal variance  $\sigma_f^2$ . We also use a linear mean function<sup>2</sup>  $\phi^\top \tilde{x}$ . and use the Direct method (McHutchon, 2014) to train the GP and estimate the noise  $\Sigma^\epsilon$  (since the observations are generated from a latent time series).

## 2.3. System Prediction

In contrast to executions, PILCO also *predicts* analytic distributions of system trajectories (Algorithm 1, line 6). It does this offline, between the online system executions, for policy evaluation. Predicted control is identical to executed control except each aforementioned quantity is instead now a random variable, distinguished with capitals:  $X_t, Z_t, U_t, \tilde{X}_t$  and  $X_{t+1}$ , all approximated as jointly Gaussian. These variables interact both in execution and prediction according to Figure 1. To predict  $X_{t+1}$  now that  $\tilde{X}_t$  is uncertain PILCO uses the iterated law of expectation and variance:

$$p(X_{t+1} | \tilde{X}_t) = \mathcal{N}(\mu_{t+1}^x, \Sigma_{t+1}^x), \quad (3)$$

$$\mu_{t+1}^x = \mathbb{E}_{\tilde{X}_t}[\mathbb{E}_f[f(\tilde{X}_t)]], \quad (4)$$

$$\Sigma_{t+1}^x = \mathbb{V}_{\tilde{X}_t}[\mathbb{E}_f[f(\tilde{X}_t)]] + \mathbb{E}_{\tilde{X}_t}[\mathbb{V}_f[f(\tilde{X}_t)]]. \quad (5)$$

<sup>1</sup> The original PILCO GP targets are relative changes in state.

<sup>2</sup> The original PILCO GP uses a zero mean function.

---

## Algorithm 1 PILCO

---

- 1: Define policy’s functional form:  $\pi : z_t \times \psi \rightarrow u_t$ .
  - 2: Initialise policy parameters  $\psi$  randomly.
  - 3: **repeat**
  - 4:   Execute system, record data.
  - 5:   Learn dynamics model.
  - 6:   Predict system trajectories from  $p(X_0)$  to  $p(X_T)$ .
  - 7:   Evaluate policy:  

$$J(\psi) = \sum_{t=0}^T \gamma^t \mathbb{E}_X[\text{cost}(X_t) | \psi].$$
  - 8:   Optimise policy:  

$$\psi \leftarrow \arg \min_{\psi} J(\psi).$$
  - 9: **until** policy parameters  $\psi$  converge
- 

After a one-step prediction from  $X_0$  to  $X_1$ , PILCO repeats the process from  $X_1$  to  $X_2$ , and up to  $X_T$ , resulting in a multi-step prediction whose joint we refer to as a distribution over system trajectories.

## 2.4. Policy Evaluation

To evaluate a policy (or more accurately, a set of policy parameters  $\psi$ ), PILCO applies a cost function to the marginal state distribution at each timestep: (Algorithm 1, line 7):

$$J(\psi) = \sum_{t=0}^T \gamma^t \mathcal{E}_t, \quad \mathcal{E}_t = \mathbb{E}_X[\text{cost}(X_t) | \psi]. \quad (6)$$

## 2.5. Policy Improvement

The policy is optimised using the analytic gradients of Eq. 6. A BFGS optimisation method searches for the set of policy parameters  $\psi$  that minimise the total cost  $J(\psi)$  using gradients information  $dJ/d\psi$  (Algorithm 1, line 8). To compute  $dJ/d\psi$  we require derivatives  $d\mathcal{E}_t/d\psi$  at each time  $t$  to chain together, and thus  $dp(S_t)/d\psi$ , detailed in PILCO (Deisenroth & Rasmussen, 2011).

## 3. PILCO Extended with Bayesian Filtering

In this section we describe the novel aspects of our method. Our method uses the same high-level algorithm as PILCO (Algorithm 1). However, we modify<sup>3</sup> two subroutines to extend PILCO into POMDPs. First, we filter observations during system execution (Algorithm 1, line 4) discussed in Section 3.1. Second, we predict system trajectories w.r.t. the filtering process (line 6), discussed in Section 3.2. Filtering maintains a belief distribution of the latent system state. The belief is conditioned on, not just the recent observation, but all previous actions and observations (Figure 2). The extra conditioning provides a less noisy input for the policy: the belief-mean instead of the raw observation  $z_t$ .

<sup>3</sup> We implement our method by modifying the PILCO source code from: <http://mlg.eng.cam.ac.uk/pilco/>.

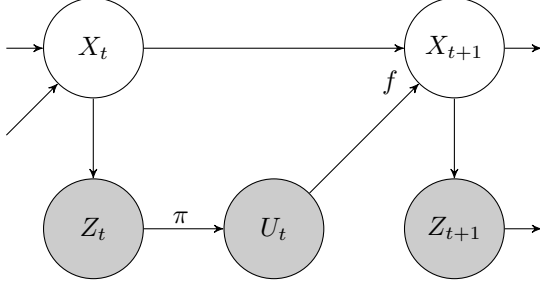


Figure 1. **The original (unfiltered) PILCO, as a directed probabilistic graphical model.** The latent system  $X_t$  is observed noisily as  $Z_t$  which is inputted directly into policy function  $\pi$  to decide action  $U_t$ . Finally, the latent system will evolve to  $X_{t+1}$ , according to the unknown, nonlinear dynamics function  $f$  of the previous state  $X_t$  and action  $U_t$ .

We continue PILCO’s distinction between *executing* the system (resulting in a single real system trajectory) and *predicting* an analytic distribution of multiple possible system trajectories. As before, during execution the system reads specific observations and decides specific actions. Under probabilistic prediction, both observations and actions are instead random variables with distributions. Our method additionally maintains an internal belief state  $b$  by filtering observations during execution. The belief is a random variable, distributed as  $b \sim \mathcal{N}(m, V)$ . Consequently, during system prediction we consider a distribution over multiple possible belief states, i.e. a distribution over random variables, which we specify with a hierarchical-distribution.

### 3.1. Filtered-System Execution

When an actual filter is applied, it starts with three pieces of information:  $m_{t|t-1}$ ,  $V_{t|t-1}$  and a noisy observation of the system  $z_t$ . The filtering ‘update step’ combines prior belief  $b_{t|t-1} \sim \mathcal{N}(m_{t|t-1}, V_{t|t-1})$  with observational likelihood  $p(x_t) = \mathcal{N}(z_t, \Sigma^\epsilon)$  to yield posterior belief  $b_{t|t}$ :

$$b_{t|t} \sim \mathcal{N}(m_{t|t}, V_{t|t}), \quad (7)$$

$$m_{t|t} = W_m m_{t|t-1} + W_z z_t, \quad (8)$$

$$V_{t|t} = W_m V_{t|t-1}, \quad (9)$$

with weight matrices  $W_m = \Sigma^\epsilon (V_{t|t-1} + \Sigma^\epsilon)^{-1}$  and  $W_z = V_{t|t-1} (V_{t|t-1} + \Sigma^\epsilon)^{-1}$ . The policy  $\pi$  is instead applied to updated belief-mean  $m_{t|t}$  (a smoother and better-informed signal than  $z_t$ ) to decide action  $u_t$ ,

$$u_t = \pi(m_{t|t}, \psi). \quad (10)$$

Thus, the joint distribution over the updated (random) belief and the (non-random) action is

$$\tilde{b}_{t|t} \doteq \begin{bmatrix} b_{t|t} \\ u_t \end{bmatrix}, \quad (11)$$

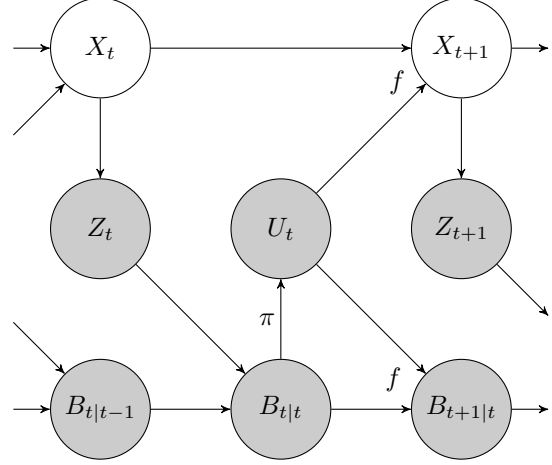


Figure 2. **Our method (PILCO extended with Bayesian filtering), as a directed probabilistic graphical model.** The latent system (top row) interacts with the agent’s belief (bottom row) via a series of observations and action decisions (middle row). At each timestep the latent system  $X_t$  is observed noisily as  $Z_t$ . The prior belief  $B_{t|t-1}$  (whose dual subscript means belief of the latent physical state at time  $t$  given all observations up until time  $t-1$  inclusive) is combined with observation  $Z_t$  resulting in posterior belief  $B_{t|t}$  (the update step). Then, the mean posterior belief  $\mathbb{E}[B_{t|t}]$  is inputted into policy function  $\pi$  to decide action  $U_t$ . Finally, the next timestep’s prior belief  $B_{t+1|t}$  is predicted using dynamics model  $f$  (the predict step).

$$\sim \mathcal{N}\left(\tilde{m}_{t|t} \doteq \begin{bmatrix} m_{t|t} \\ u_t \end{bmatrix}, \tilde{V}_{t|t} \doteq \begin{bmatrix} V_{t|t} & 0 \\ 0 & 0 \end{bmatrix}\right).$$

Finally, the filtering ‘prediction step’ computes  $p(b_{t+1|t})$  as approximately the output of dynamics model  $f$  with uncertain input  $\tilde{b}_{t|t}$ . The output distribution  $p(f(\tilde{b}_{t|t}))$  is non-Gaussian and intractable, yet has analytically solvable moments (Deisenroth & Rasmussen, 2011). We approximate the distribution  $p(b_{t+1|t})$  as Gaussian using moment-matching for tractability:

$$b_{t+1|t} \sim \mathcal{N}(m_{t+1|t}, V_{t+1|t}), \quad (12)$$

$$m_{t+1|t}^a = \mathbb{E}_{\tilde{b}_{t|t}}[f^a(\tilde{b}_{t|t})], \quad (13)$$

$$V_{t+1|t}^{ab} = \mathbb{C}_{\tilde{b}_{t|t}}[f^a(\tilde{b}_{t|t}), f^b(\tilde{b}_{t|t})], \quad (14)$$

where  $m_{t+1|t}^a$  and  $V_{t+1|t}^{ab}$  are derived in Appendix A. The process then repeats using the predictive belief (Eq. 12-14) as the prior belief in the following timestep. This completes the specification of the system in execution.

### 3.2. Filtered-System Prediction

In *system prediction*, we compute the probabilistic behaviour of the filtered system via an analytic distribution of possible beliefs. A distribution over beliefs  $b$  is in principle a distribution over its parameters  $m$  and  $V$ . To distinguish

$m$  and  $b$  as now being *random* and *hierarchically-random* respectively, we capitalise them:  $M$  and  $B$ . As an approximation we are going to assume that the distribution on the variance  $V_{t|t-1}$  is a delta function (i.e. some fixed value, for a given timestep). Restricting  $M$  to being Gaussian distributed then we begin system prediction with the joint:

$$\begin{bmatrix} M_{t|t-1} \\ Z_t \end{bmatrix} \sim \mathcal{N} \left( \begin{bmatrix} \mu_{t|t-1}^m \\ \mu_t^x \end{bmatrix}, \begin{bmatrix} \Sigma_{t|t-1}^m & 0 \\ 0 & \Sigma_t^z \end{bmatrix} \right), \quad (15)$$

where  $\Sigma_t^z = \Sigma_t^x + \Sigma_t^e$ .

**Remark:** We now pause for a moment to reflect on the full model of the filtered system (Figure 2). The model is slightly more general than a POMDP. For instance, it can predict the consequences of a mismatch between the latent state  $X_t$  and the agent’s belief  $B_{t|t-1}$ . Such a feature is perhaps not very interesting, however, since from the agent’s point of view, the latent state is unknown. All the agent’s knowledge of the latent state is summarised by its belief. A special case of our framework that reduces exactly to a POMDP is as follows. We constrain the latent state distribution to be a ‘flattened’ version of the hierarchically-distributed belief:  $X_t \sim \mathcal{N}(\mu_t^x, \Sigma_t^x)$ , where  $\mu_t^x = \mu_{t|t-1}^m$  and  $\Sigma_t^x = \Sigma_{t|t-1}^m + V_{t|t-1}$ . Additionally we use identical dynamics function  $f$  for both latent and belief dynamics. Doing so, the Markov system state in Figure 2 reduces from  $\{X_t, B_{t|t-1}\}$  to just  $\{B_{t|t-1}\}$ . I.e. predicting the next latent state  $X_{t+1} \sim \mathcal{N}(\mu_{t+1}^x, \Sigma_{t+1}^x)$  is conditionally independent of  $X_t$  given  $B_{t|t-1}$ . In such case,  $p(X_{t+1})$  does not need to be explicitly computed, since an analogous relationship holds true:  $\mu_{t+1}^x = \mu_{t+1|t}^m$  and  $\Sigma_{t+1}^x = \Sigma_{t+1|t}^m + V_{t+1|t}$ . We will use this special POMDP case throughout the rest of this paper for system prediction. Multi-step prediction, which requires a Markov state from one timestep to the next, now simply predicts from one set of beliefs to the next. This is the belief-MDP interpretation of POMDPs (Kaelbling et al., 1998).

Moving on, the updated belief posterior is also Gaussian,

$$M_{t|t} \sim \mathcal{N} \left( \mu_{t|t}^m, \Sigma_{t|t}^m \right), \quad (16)$$

where  $\mu_{t|t}^m = \mu_{t|t-1}^m$  and  $\Sigma_{t|t}^m = W_m \Sigma_{t|t-1}^m W_m^\top + W_z \Sigma_t^z W_z^\top$ . The policy now has a random input  $M_{t|t}$ , thus the control output must also be random (even though we use a deterministic policy function):

$$U_t = \pi(M_{t|t}, \psi), \quad (17)$$

which we implement by overloading the policy function:

$$(\mu_t^u, \Sigma_t^u, C_t^{mu}) = \pi(\mu_{t|t}^m, \Sigma_{t|t}^m, \psi), \quad (18)$$

where  $\mu_t^u$  is the output mean,  $\Sigma_t^u$  the output variance and  $C_t^{mu}$  input-output covariance with premultiplied inverse

input variance,  $C_t^{mu} \doteq (\Sigma_{t|t}^m)^{-1} \mathbb{C}_M[M_{t|t}, U_t]$ . Making a moment-matched approximation yields a joint Gaussian:

$$\tilde{M}_{t|t} \doteq \begin{bmatrix} M_{t|t} \\ U_t \end{bmatrix} \quad (19)$$

$$\sim \mathcal{N} \left( \mu_{t|t}^{\tilde{m}} \doteq \begin{bmatrix} \mu_{t|t}^m \\ \mu_t^u \end{bmatrix}, \Sigma_{t|t}^{\tilde{m}} \doteq \begin{bmatrix} \Sigma_{t|t}^m & \Sigma_{t|t}^m C_t^{mu} \\ (C_t^{mu})^\top \Sigma_{t|t}^m & \Sigma_t^u \end{bmatrix} \right) \quad (20)$$

Finally, we probabilistically predict 1) the belief-mean distribution  $p(M_{t+1|t})$  and 2) the expected belief-variance  $\bar{V}_{t+1|t} = \mathbb{E}[V_{t+1|t}]$ , both detailed in Appendix B. We have now discussed the one-step prediction of the filtered system, from  $B_{t|t-1}$  to  $B_{t+1|t}$ . Using this process repeatedly, from initial belief  $B_{0|0}$  we predict forwards to  $B_{1|0}$ , then to  $B_{2|1}$  etc., up to  $B_{T|T-1}$ .

### 3.3. Policy Evaluation and Improvement

To evaluate a policy we again apply the cost function (Eq. 6) to the multi-step prediction (Section 3.2). Note the marginal distribution of each latent state  $X_t$  at time  $t$  is related to the belief  $B_{t|t-1}$  by:

$$X_t \sim \mathcal{N}(\mu_{t|t-1}^m, \Sigma_{t|t-1}^m + V_{t|t-1}) \quad \forall t, \quad (21)$$

where the belief is hierarchically distributed:  $B_{t|t-1} \sim \mathcal{N}(M_{t|t-1}, V_{t|t-1}) \sim \mathcal{N}(\mathcal{N}(\mu_{t|t-1}^m, \Sigma_{t|t-1}^m), V_{t|t-1})$ . The policy is again optimised using the analytic gradients of Eq. 6, except now we consider how filtering affects the gradients of  $X_t$ . Let  $\text{vec}(\cdot)$  be the ‘unwrap operator’ that reshapes a matrix into a vector. We can define a Markov filtered-system from the belief’s parameters:  $S_t = [M_{t|t-1}^\top, \text{vec}(V_{t|t-1})^\top]^\top$ . To predict system evolution, the state distribution is defined (further details in Appendix C):

$$p(S_t) \sim \mathcal{N} \left( \mu_t^s = \begin{bmatrix} \mu_{t|t-1}^m \\ \text{vec}(V_{t+1|t}) \end{bmatrix}, \Sigma_t^s = \begin{bmatrix} \Sigma_{t|t-1}^m & 0 \\ 0 & 0 \end{bmatrix} \right). \quad (22)$$

## 4. Experiments

We test our algorithm on the cartpole swing-up problem (Figure 3), a benchmark for comparing controllers of non-linear dynamical systems. We experiment using a physics simulator by solving the differential equations of the system. The pendulum begins each episode hanging downwards with the goal of swinging it up and stabilising it.

We now describe our test system. The cart has mass  $m_c = 0.5\text{kg}$ . A zero-order hold controller applies horizontal forces to the cart within range  $[-10, 10]\text{N}$ . The controller / policy is a radial basis function with 100 centroids. Friction resists the cart’s motion with damping coefficient  $b = 0.1\text{Ns/m}$ . Connected to the cart is a pole of length  $l = 0.2\text{m}$  and mass  $m_p = 0.5\text{kg}$  located at its endpoint, which swings due to gravity’s acceleration  $g = 9.82\text{m/s}^2$ .

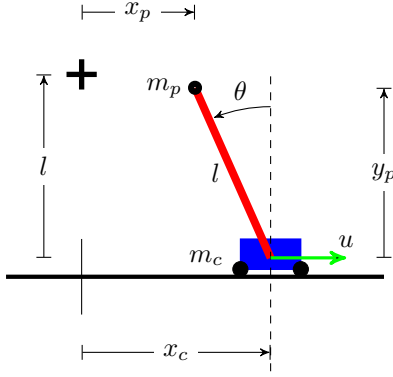


**Figure 3. The cartpole swing-up task.** A pendulum of length  $l$  is attached to a cart by a frictionless pivot. The cart has mass  $m_c$  and position  $x_c$ . The pendulum’s endpoint has mass  $m_p$  and position  $(x_p, y_p)$ , with angle  $\theta$  from vertical. The system begins with cart at position  $x_c = 0$  and pendulum hanging down:  $\theta = \pi$ . The goal is to accelerate the cart by applying horizontal force  $u_t$  at each timestep  $t$  to invert then stabilise the pendulum’s endpoint at the goal (black cross), i.e. to maintain  $x_c = 0$  and  $\theta = 0$ .

An inexpensive camera observes the system. Frame rates of \$10 webcams are typically 30Hz at maximum resolution, thus the time discretisation is  $\Delta t = 1/30s$ . The state  $x$  comprises the cart position, pendulum angle, and their time derivatives  $x = [x_c, \theta, \dot{x}_c, \dot{\theta}]^\top$ . The cartpole’s motion is described with the differential equation:

$$\dot{x} = \begin{bmatrix} \dot{x}_c \\ \dot{\theta} \\ \frac{-2m_p l \dot{\theta}^2 s + 3m_p g s c + 4u - 4b \dot{x}_c}{4(m_c + m_p) - 3m_p c^2} \\ \frac{-3m_p l \dot{\theta}^2 s c + 6(m_c + m_p) g s + 6(u - b \dot{x}_c) c}{4l(m_c + m_p) - 3m_p l c^2} \end{bmatrix}, \quad (23)$$

using shorthand  $s = \sin \theta$  and  $c = \cos \theta$ . Both the initial latent state and initial belief are i.i.d.:  $X_0, B_{0|0} \stackrel{iid}{\sim} \mathcal{N}(M_{0|0}, V_{0|0})$  where  $M_{0|0} \sim \delta([0, \pi, 0, 0]^\top)$  and  $V_{0|0}^{\frac{1}{2}} = \text{diag}([0.2m, 0.2rad, 0.2m/s, 0.2rad/s])$ .

The camera’s noise standard deviation is:  $(\Sigma^\epsilon)^{\frac{1}{2}} = \text{diag}([0.03m, 0.03rad, \frac{0.03}{\Delta t} m/s, \frac{0.03}{\Delta t} rad/s])$ , noting  $0.03rad \approx 1.7^\circ$ . We use the  $\frac{0.03}{\Delta t}$  terms since using a camera we cannot observe velocities directly but can estimate with finite differences, and thus the observation error is dependent on the observation error of the positions. Each episode has a two second time horizon (60 timesteps). The cost function we impose is  $1 - \exp(-\frac{1}{2}d^2/\sigma_c^2)$  where  $\sigma_c = 0.25m$  and  $d^2$  is the squared Euclidean distance between the pendulum’s endpoint  $(x_p, y_p)$  and its goal  $(0, l)$ . I.e.  $d^2 = x_p^2 + (l - y_p)^2 = (x_c - l \sin \theta)^2 + (l - l \cos \theta)^2$ .

We compare four algorithms: 1) PILCO (Deisenroth & Rasmussen, 2011) as a baseline (unfiltered execution, and unfiltered full-prediction); 2) the method

by (Dallaire et al., 2009) (filtered execution, and filtered MAP-prediction); 3) the method by (Deisenroth & Peters, 2012) (filtered execution, and unfiltered full-prediction); and lastly 4) our method (filtered execution, and filtered full-prediction). For clear comparison we opted for a tightly controlled experiment. We control for data and dynamics models, i.e. each algorithm has access to the exact same data and exact same dynamics model. The reason is to eliminate variance in performance caused by different algorithms choosing different actions. We generate a single dataset by running the baseline PILCO algorithm for 11 episodes (totalling 22 seconds of system interaction). The independent variables of our experiment are 1) the method of system prediction and 2) the method of system execution. We then optimise each policy from the same initialisation using their respective prediction methods. Finally, we measure and compare their performances in both prediction and execution.

## 5. Results and Analysis

We now compare algorithm performance, both predictive (Figure 4) and from empirical execution (Figure 5).

### 5.1. Predictive Performance

First, we analyse predictive costs per timestep (Figure 4). Since predictions are probabilistic, the costs have distributions, with the exception of Dallaire et al. (2009) which predicts MAP trajectories and therefore has deterministic cost. Even though we plot distributed costs, policies are optimised w.r.t. expected total cost only. Using the same dynamics, the different prediction methods optimise different policies (with the exception of (Deisenroth & Rasmussen, 2011) and (Deisenroth & Peters, 2012), whose prediction methods are identical). During the first 10 timesteps, we note identical performance with maximum cost due to the non-zero time required physically swing the pendulum up near the goal. Performances thereafter diverge. Since we predict w.r.t. a filtering process, less noise is predicted to be injected into the policy, and the optimiser can thus afford higher gain parameters w.r.t. the pole at balance point. If we linearise our policy around the goal point, our policy has a gain of  $-81.7N/rad$  w.r.t. pendulum angle, a larger-magnitude than both Deisenroth method gains of  $-39.1N/rad$  (negative values refer to *left* forces in Figure 3). Being afforded higher gains our policy is more reactive and more likely to catch a falling pendulum. Finally, we note Dallaire et al. (2009) predict very high performance. Without balancing the costs across multiple possible trajectories, the method instead optimises a sequence of deterministic states to near perfection.

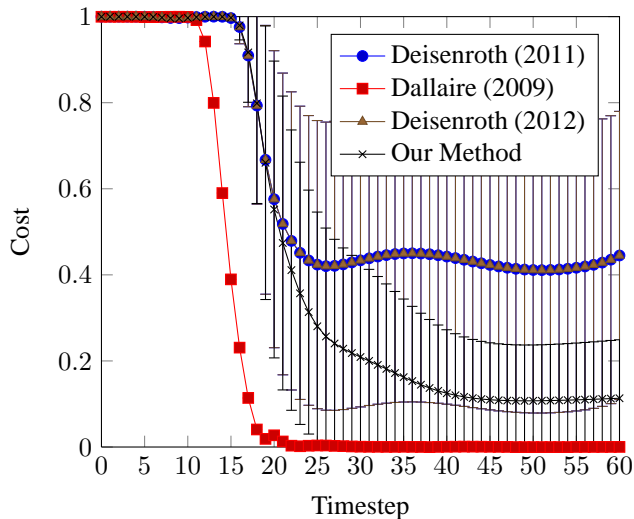


Figure 4. **Predictive costs per timestep.** The error bars show  $\pm 1$  standard deviation. Each algorithm has access to the same data set (generated by baseline Deisenroth (2011)) and the same dynamics model. Algorithms differ in their multi-step prediction methods (except Deisenroth’s algorithms whose predictions thus overlap).

## 5.2. Empirical Performance

We now compare the predictive results against the empirical results, using 100 executions of each algorithm (Figure 5). First, we notice a stark difference between predictive and executed performances from (Dallaire et al., 2009), due to neglecting model uncertainty, suffering model bias. In contrast, the other methods consider uncertainty and have relatively unbiased predictions, judging by the similarity between predictive-vs-empirical performances. Deisenroth’s methods, which differ only in execution, illustrate that filtering during execution-only can be better than no filtering at all. However, the real benefit comes when the policy is evaluated from multi-step predictions of a filtered system. Opposed to Deisenroth & Peters’s method (2012), our method’s predictions reflect reality closer because we both predict and execute system trajectories using closed loop filtering control.

## 6. Conclusion and Future Work

In this paper, we extended the original PILCO algorithm (Deisenroth & Rasmussen, 2011) to filter observations, both during system execution and multi-step probabilistic prediction required for policy evaluation. The extended framework enables learning in *partially-observed* environments (POMDPs) whilst retaining PILCO’s data-efficiency property. We demonstrated successful application to a benchmark control problem, the noisily-observed cartpole swing-up. Our algorithm learned a good policy under significant observation noise in less than 30 seconds of system interaction. Importantly, our algorithm evaluates

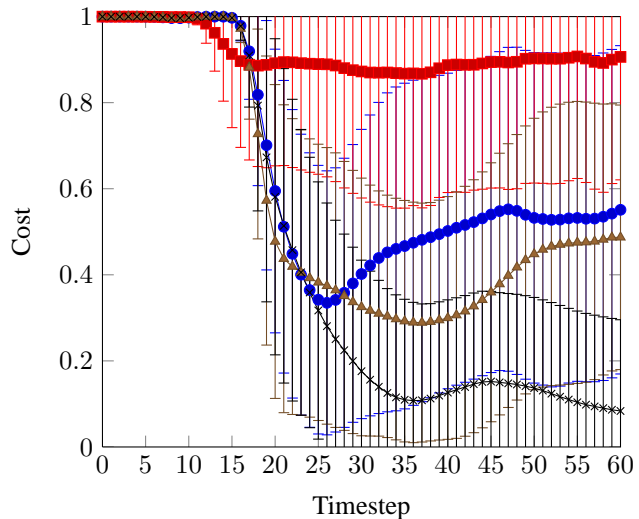


Figure 5. **Empirical costs per timestep.** We generate empirical cost distributions from 100 executions per algorithm. Error bars show  $\pm 1$  standard deviation. The plot colours and shapes correspond to the legend in Figure 4.

policies with predictions that are faithful to reality. We predict w.r.t. closed loop filtered control precisely because we execute closed loop filtered control.

We showed experimentally that *faithful* and *probabilistic* predictions give greater performance gains than otherwise. For clear comparison we constrained each algorithm to use the same dynamics dataset rather than each interacting with the system to generate their own. If we relaxed this experimental constraint, we anticipate our method’s performance gains would be greater still. However, the extra variance in empirical performance (caused by selection of different data) means a much larger number of experiments is required to test if such an *additional* performance gain exists, which we plan to do in future work.

Several more challenges remain for future work. Firstly the assumption of zero variance of the belief-variance could be relaxed. A relaxation allows distributed trajectories to more accurately consider belief states having various degrees of certainty (belief-variance). E.g. system trajectories have larger belief-variance when passing through data-sparse regions of state-space, and smaller belief-variance in data-dense regions. Secondly, the policy could be a function of the full belief distribution (mean and variance) rather than just the mean. Such flexibility could help the policy make more ‘cautious’ actions when more uncertain about the state. Thirdly, the framework could be extended to active learning. Currently, the framework is a passive learner, greedily optimising the total cost-means and ignoring cost-variance information which could otherwise better inform exploration, increasing data-efficiency further.

## A. Dynamics Predictions in System-Execution

Here we specify the predictive distribution  $p(b_{t+1|t})$ , whose moments are equal to the moments from dynamics model output  $f$  with uncertain input  $\tilde{b}_{t|t}$ :

$$b_{t+1|t} \sim \mathcal{N}(m_{t+1|t}, V_{t+1|t}), \quad (24)$$

$$m_{t+1|t}^a = \mathbb{E}_{\tilde{b}_{t|t}}[f^a(\tilde{b}_{t|t})] = s_a^2 \beta_a^\top q^a + \phi^\top \tilde{m}_{t|t}, \quad (25)$$

$$\begin{aligned} C_a &= \tilde{V}_{t|t}^{-1} \mathbb{C}_{\tilde{b}_{t|t}}[f^a(\tilde{b}_{t|t}) - \phi^\top \tilde{b}_{t|t}], \\ &= s_a^2 (\Lambda_a + \tilde{V}_{t|t})^{-1} (x - \tilde{m}_{t|t}) \beta_a q^a, \end{aligned} \quad (26)$$

$$\begin{aligned} V_{t+1|t}^{ab} &= \mathbb{C}_{\tilde{b}_{t|t}}[f^a(\tilde{b}_{t|t}), f^b(\tilde{b}_{t|t})], \\ &= s_a^2 s_b^2 [\beta_a^\top (Q^{ab} - q^a q^{b\top}) \beta_b + \\ &\quad \delta_{ab} (s_a^{-2} - \text{tr}((K_a + \Sigma_\varepsilon^a)^{-1} Q^{aa}))] + \\ &\quad C_a^\top \tilde{V}_{t|t} \phi_b + \phi_a^\top \tilde{V}_{t|t} C_b + \phi_a^\top \tilde{V}_{t|t} \phi_b, \end{aligned} \quad (27)$$

$$q_i^a = q(x_i, \tilde{m}_{t|t}, \Lambda_a, \tilde{V}_{t|t}), \quad (28)$$

$$Q_{ij}^{ab} = Q(x_i, x_j, \Lambda_a, \Lambda_b, 0, \tilde{m}_{t|t}, \tilde{V}_{t|t}). \quad (29)$$

where,

$$\begin{aligned} q(x_i, \mu, \Lambda, V) &\doteq |\Lambda^{-1}V + I|^{-1/2} \\ &\times \exp\left(-\frac{1}{2}(x_i - \mu)[\Lambda + V]^{-1}(x_i - \mu)\right), \end{aligned} \quad (30)$$

$$\begin{aligned} Q(x_i, x_j, \Lambda_a, \Lambda_b, V, \mu, \Sigma) &\doteq |R|^{-1/2} \\ &\times q(x_i, \mu, \Lambda_a, V) q(x_j, \mu, \Lambda_b, V) \\ &\times \exp\left(\frac{1}{2}z_{ij}^\top R^{-1} \Sigma z_{ij}\right), \end{aligned} \quad (31)$$

$$R = \Sigma((\Lambda_a + V)^{-1} + (\Lambda_b + V)^{-1}) + I, \quad (32)$$

$$z_{ij} = (\Lambda_a + V)^{-1}(x_i - \mu) + (\Lambda_b + V)^{-1}(x_j - \mu), \quad (33)$$

$$\beta_a = (K_a + \Sigma^{\varepsilon, a})^{-1}(y_a - \phi_a^\top x), \quad (34)$$

and training inputs are  $x$ , outputs are  $y_a$ , and the GP linear mean function has weight-vector  $\phi \in \mathbb{R}^D$ .

## B. Dynamics Predictions in System-Prediction

Here we describe the prediction formulae for the random belief state in system-prediction. We again note, during execution, our belief distribution is specified by certain parameters,  $b_{t|t} \sim \mathcal{N}(m_{t|t}, V_{t|t})$ . By contrast, during system prediction, our belief distribution is specified by an uncertain belief-mean and certain belief-variance:  $B_{t|t} \sim \mathcal{N}(M_{t|t}, V_{t|t}) \sim \mathcal{N}(\mathcal{N}(\mu_{t|t}^m, \Sigma_{t|t}^m), \tilde{V}_{t|t})$ , where we assumed a delta distribution on  $V$ :  $\text{vec}(V_{t|t}) \sim \mathcal{N}(\text{vec}(\tilde{V}_{t|t}), 0)$  for mathematical simplicity. Therefore we conduct GP prediction given hierarchically-uncertain inputs, giving rise to the various subsection below:

### B.1. Mean of the Belief-Mean

Dynamics prediction uses input  $\tilde{M}_{t|t} \sim \mathcal{N}(\mu_{t|t}^m, \Sigma_{t|t}^m)$ , which is jointly distributed according to Eq. 19-20. Using the belief-mean  $m_{t+1|t}^a$  definition (Eq. 25),

$$\mu_{t+1|t}^{m,a} = \mathbb{E}_{\tilde{M}_{t|t}}[M_{t+1|t}^a],$$

$$\begin{aligned} &= \int M_{t+1|t}^a \mathcal{N}(\tilde{M}_{t|t} | \mu_{t|t}^m, \Sigma_{t|t}^m) d\tilde{M}_{t|t}, \\ &= s_a^2 \beta_a^\top \hat{q}^a, \end{aligned} \quad (35)$$

$$\hat{q}_i^a = q(x_i, \mu_{t|t}^m, \Lambda_a, \Sigma_{t|t}^m + \tilde{V}_{t|t}). \quad (36)$$

### B.2. Input-Output Covariance

The expected input-output covariance belief term (Eq. 26) (also the input-output covariance of the belief-mean) is:

$$\begin{aligned} \hat{C}_a &= \tilde{V}_{t|t}^{-1} \mathbb{E}_{\tilde{M}_{t|t}}[\mathbb{C}_{B_{t|t}}[\tilde{B}_{t|t}, f(\tilde{B}_{t|t}) - \phi_a^\top \tilde{M}_{t|t}]], \\ &= (\Sigma_{t|t}^m)^{-1} \mathbb{C}_{\tilde{M}_{t|t}}[\tilde{M}_{t|t}, \mathbb{E}_{B_{t|t}}[f(\tilde{B}_{t|t}) - \phi_a^\top \tilde{M}_{t|t}]], \\ &= s_a^2 (\Lambda_a + \Sigma_{t|t}^m + \tilde{V}_{t|t})^{-1} (x - \mu_{t|t}^m) \beta_a \hat{q}_i^a. \end{aligned} \quad (37)$$

### B.3. Variance of the Belief-Mean

The variance of randomised belief-mean (Eq 25) is:

$$\begin{aligned} \Sigma_{t+1|t}^{m,ab} &= \mathbb{C}_{\tilde{M}_{t|t}}[M_{t+1|t}^a, M_{t+1|t}^b], \\ &= \int M_{t+1|t}^a M_{t+1|t}^b \mathcal{N}(\tilde{M}_{t|t} | \mu_{t|t}^m, \Sigma_{t|t}^m) d\tilde{M}_{t|t} - \\ &\quad \mu_{m_{t+1|t}}^a \mu_{m_{t+1|t}}^b, \\ &= s_a^2 s_b^2 \beta_a^\top (\hat{Q}^{ab} - \hat{q}^a \hat{q}^{b\top}) \beta_b + \\ &\quad \hat{C}_a^\top \Sigma_{t|t}^m \phi_b + \phi_a^\top \Sigma_{t|t}^m \hat{C}_b + \phi_a^\top \Sigma_{t|t}^m \phi_b, \end{aligned} \quad (38)$$

$$\hat{Q}_{ij}^{ab} = Q(x_i, x_j, \Lambda_a, \Lambda_b, \tilde{V}_{t|t}, \mu_{t|t}^m, \Sigma_{t|t}^m). \quad (39)$$

### B.4. Mean of the Belief-Variance

Using the belief-variance  $V_{t+1|t}^{ab}$  definition (Eq. 27),

$$\begin{aligned} \tilde{V}_{t+1|t}^{ab} &= \mathbb{E}_{\tilde{M}_{t|t}}[V_{t+1|t}^{ab}], \\ &= \int V_{t+1|t}^{ab} \mathcal{N}(\tilde{M}_{t|t} | \mu_{t|t}^m, \Sigma_{t|t}^m) d\tilde{M}_{t|t}, \\ &= s_a^2 s_b^2 [\beta_a^\top (\tilde{Q}^{ab} - \hat{Q}^{ab}) \beta_b + \\ &\quad \delta_{ab} (s_a^{-2} - \text{tr}((K_a + \Sigma_\varepsilon^a)^{-1} \tilde{Q}^{aa}))] + \\ &\quad \tilde{C}_a^\top \tilde{V}_{t|t} \phi_b + \phi_a^\top \tilde{V}_{t|t} \tilde{C}_b + \phi_a^\top \tilde{V}_{t|t} \phi_b, \end{aligned} \quad (40)$$

$$\tilde{Q}_{ij}^{ab} = Q(x_i, x_j, \Lambda_a, \Lambda_b, 0, \mu_{t|t}^m, \Sigma_{t|t}^m + \tilde{V}_{t|t}). \quad (41)$$

## C. Gradients for Policy Improvement

To compute policy gradient  $dJ/d\psi$  we first require  $d\mathcal{E}_t/d\psi$ :

$$\begin{aligned} \frac{d\mathcal{E}_t}{d\theta} &= \frac{d\mathcal{E}_t}{dp(S_t)} \frac{dp(S_t)}{d\theta}, \\ &= \frac{d\mathcal{E}_t}{\partial \mu_t^s} \frac{\partial \mu_t^s}{d\theta} + \frac{d\mathcal{E}_t}{\partial \Sigma_t^s} \frac{\partial \Sigma_t^s}{d\theta}, \end{aligned} \quad (42)$$

and

$$\frac{dp(S_{t+1})}{d\theta} = \frac{dp(S_{t+1})}{dp(S_t)} \frac{dp(S_t)}{d\theta} + \frac{\partial p(S_{t+1})}{\partial \theta}. \quad (43)$$

Application of the chain rule backwards from the state distribution at the horizon  $S_T$ , to  $S_t$  at arbitrary time  $t$ , is analogous to that detailed in PILCO (Deisenroth & Rasmussen, 2011), where we use  $S_t$ ,  $\mu_t^s$  and  $\Sigma_t^s$  in the place of  $x_t$ ,  $\mu_t$  and  $\Sigma_t$  respectively.



## References

- Dallaire, P., Besse, C., Ross, S., and Chaib-Draa, B. Bayesian reinforcement learning in continuous POMDPs with Gaussian processes. In *International Conference on Intelligent Robots and Systems (IROS 2009)*, pp. 2604–2609. IEEE, 2009.
- Deisenroth, M. and Peters, J. Solving nonlinear continuous state-action-observation POMDPs for mechanical systems with Gaussian noise. In *European Workshop on Reinforcement Learning (EWRL 2012)*, 2012.
- Deisenroth, M. and Rasmussen, C. PILCO: A model-based and data-efficient approach to policy search. In *International Conference on Machine Learning (ICML 2011)*, pp. 465–472, New York, NY, USA, 2011.
- Kaelbling, L., Littman, M., and Cassandra, A. Planning and acting in partially observable stochastic domains. *Artificial intelligence*, 101(1):99–134, 1998.
- Ko, J. and Fox, D. GP-BayesFilters: Bayesian filtering using Gaussian process prediction and observation models. *Autonomous Robots*, 27(1):75–90, 2009.
- McHutchon, A. *Nonlinear modelling and control using Gaussian processes*. PhD thesis, Department of Engineering, University of Cambridge, 2014.
- Ross, S., Chaib-Draa, B., and Pineau, J. Bayesian reinforcement learning in continuous POMDPs with application to robot navigation. In *International Conference on Robotics and Automation (ICRA 2008)*, pp. 2845–2851. IEEE, 2008.
- Smallwood, R. and Sondik, E. The optimal control of partially observable Markov processes over a finite horizon. *Operations Research*, 21(5):1071–1088, 1973.